Non-Markovian nature of exciton-exciton scattering in a GaAs single quantum well observed by phase-locked laser pulses

Y. Ogawa, H. Tahara, and F. Minami
Department of Physics, Tokyo Institute of Technology, Oh-Okayama 2-12-1, Tokyo 152-8551, Japan
(Received 26 November 2012; published 23 April 2013)

We report the non-Markovian nature of heavy hole-heavy hole and heavy hole-light hole exciton scattering in a GaAs single quantum well. The homogeneous width depends on the exciton population, which is controlled by the delay time of phase-locked pulses. This effect is explained on the basis of excitation-induced dephasing in Markovian approximation. For short times, the homogeneous width decreases and deviates from the Markovian behavior, due to the non-Markovian behavior of the exciton-exciton scattering. We analyze the homogeneous width by using a weakly interacting boson model including the non-Markovian effect. The correlation time of the exciton-exciton scattering is estimated as 0.43 ps.

DOI: 10.1103/PhysRevB.87.165305 PACS number(s): 78.47.jf, 42.65.Sf, 71.35.Gg, 78.67.De

An ideal model system for the investigation of many-body physics is an optically excited semiconductor whose optical properties are governed by excitonic resonances.[1] The many-body interaction of photoexcited carriers leads to rich phenomena such as the formation of the excitonic molecule,[2] exciton-Mott transition,[3] and Bose-Einstein condensation.[4] Theoretical approaches to analyze the many-body interaction, e.g., nonequilibrium Green's function method[5] and the dynamics controlled truncation approach,[6] have been developed in step with the progress of the experiment.

In general, the many-body interaction does not occur instantaneously but depends on the past history of scattering. The time scale that reflects the duration for which the past interaction influences the present dynamics is referred to as the correlation time of the interaction, and such dynamics are considered to be non-Markovian. When the time scale of measurement corresponds to the correlation time of interactions, the non-Markovian dynamics can be observed. The non-Markovian effect is an important topic for the study of many-body interactions.

Many-body interactions of excitons in semiconductors are commonly probed by nonlinear optical spectroscopy. Transient four-wave mixing (FWM) has been employed for investigating the non-Markovian effects that mainly originate from exciton-optical phonon interaction[7–11] and exciton-acoustic phonon interaction.[12–18] In contrast, there are only a few reports on the non-Markovian behavior induced by exciton-exciton scattering.[15,19] The reason for the scarcity of research is that the correlation time of exciton-exciton scattering is short as compared to that of exciton-phonon scattering, and the method for the measurement of the non-Markovian behavior of exciton-exciton scattering is not well established.

In this paper we show that coherent control is a versatile tool to observe the non-Markovian effect of the exciton-exciton scattering and we discuss the correlation time in a GaAs single quantum well (SQW) by using FWM measurements. First, we introduce the sample that shows a clear excitation density dependence of the peak energy and linewidth of the FWM spectrum. Next, we show the results of the coherent control of the FWM signal by using a phase-locked pulse pair. A heavy hole (hh)-light hole (lh) quantum beat disappears with the changing of the delay time of phase-locked pulses because of polarization interference. The offset of the diffracted signal oscillates due to the quantum beat of a fifth-order nonlinear signal. Finally, we demonstrate that the dephasing time is controlled by changing the delay time of phase-locked pulses, which is the result of the modulation of exciton population. We observe the non-Markovian behavior of the exciton-exciton scattering. The correlation time is estimated by using a weakly interacting boson model.

A mode-locked Ti:sapphire laser (100 fs, 76 MHz) was used as the light source. An actively stabilized Michelson interferometer produced two phase-locked pulses $k_{1'}$ and k_1, with a temporal separation of $t_{1'1}$ as shown in Fig. 1. The length of one arm of the Michelson interferometer was controlled in order to maintain a constructive (in-phase) interference at the hh exciton energy. Another pulse k_2, with delay time t_{12}, interacts with the phase-locked pulses $k_{1'}$ and k_1. We observed diffracted signals in the $2k_2$-k_1 direction. In the $\chi^{(3)}$ regime, the diffracted signal is the linear addition of the FWM signals in the $2k_2$-k_1 and $2k_2$-$k_{1'}$ directions. In the $\chi^{(5)}$ regime, the diffracted signal contains the six-wave mixing (SWM) signal in the same diffracted direction $2k_2$-$2k_1 + k_{1'}$. All beams had the same intensity (0.08–3.2 mW), and the polarization was controlled by wave plates and polarizers. The polarization of the detected signal was not selected. All measurements were performed on a GaAs SQW with a well thickness of 15 nm at 4 K. The photon energy of the laser light was resonant with the hh and lh excitons.

Excitation density dependencies of the time-integrated (TI) and spectrally resolved (SR) FWM signal intensity at $t_{1'1} = 0$ ps are shown in Figs. 2(a) and 2(b), respectively. The dephasing time decreases with the increase in the excitation density as a result of the excitation-induced dephasing (EID) process.[20] Because the inhomogeneous width of the sample is much smaller than the width obtained at the high excitation density, EID is observed in the SR-FWM. At the lowest excitation density, a sharp spectrum of the hh exciton resonance with a full width at half maximum of 0.446 meV was observed. The spectral width asymmetrically broadens with the increase in the excitation density. Figure 2(c) indicates the excitation density dependence of the homogeneous width of the hh exciton peak estimated from the decay rate and spectral width. In this estimation we assumed no inhomogeneous broadening.

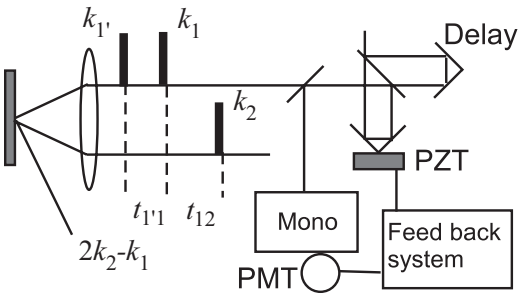

FIG. 1. Schematic of the experimental setup. Pulses k_1 and $k_{1'}$ of the temporal separation $t_{1'1}$ are phase-locked constructively at a heavy hole exciton energy. The diffracted signals in the $2k_2$-k_1 direction are detected. Mono: monochromator, PMT: photomultiplier tube, PZT: piezo-electric actuator.

The homogeneous width increases linearly at low excitation density.

The peak energy of the hh exciton indicates a blue shift with the increase in the excitation density, as shown in Fig. 2(d). The excitation-induced shift (EIS) is determined by the conflict between the band-gap renormalization and the reduction of the exciton binding energy due to the screening of the Coulomb potential. There is no shift in the bulk samples due to this compensation.[5] As the reduction in dimensionality leads to a reduction of the Coulomb interaction, a blue shift occurs at resonant excitation and under a low temperature condition in quantum wells.[21,22]

Figures 3(a)–3(d) show the FWM intensity as a function of t_{12} and $t_{1'1}$ measured at several experimental conditions. Here "RRR" refers to the configuration where $k_{1'}$, k_1, and k_2 pulses are co-circular polarized and "RLV" where $k_{1'}$ and k_1 pulses are cross-circular polarized and k_2 pulse is linear polarized. "High" and "low" denote high and low excitation densities, respectively. The FWM intensities at $t_{1'1} = 0$, 0.33, and 0.66 ps are shown in Figs. 3(e) and 3(f). A conventional two-pulse FWM signal is observed at $t_{1'1} = 0$ ps, which shows the hh-lh quantum beat with a period of 0.66 ps. The hh-lh quantum beat disappears at $t_{1'1} = 0.33$, 0.99, 1.66, and 2.33 ps due to the interference in antiphase between the third-order nonlinear polarizations in $2k_2$-$k_{1'}$ and $2k_2$-k_1 directions: $P^{(3)}_{2k_2-k_{1'}}$ and $P^{(3)}_{2k_2-k_1}$. The condition of the disappearance is $t_{1'1} = 2\pi(n + 1/2)/\Delta\omega$, where n is an integer and $\hbar\Delta\omega$ is the energy difference between hh and lh excitons. The period of the disappearance is equal to that of the hh-lh quantum beat $2\pi/\Delta\omega$, which corresponds to the experimental results. The hh-lh quantum beat disappears in both RRR and RLV configurations due to the polarization interference.

The offset of the diffracted signal increases at $t_{1'1} = 0.33$, 0.99, 1.66, and 2.33 ps only for the RRR configuration. In the $\chi^{(5)}$ regime, the diffracted signal contains the SWM signal in the same diffracted direction $2k_2$-$2k_1 + k_{1'}$ for the RRR configuration. Note that there is no SWM signal in the $2k_2$-$2k_{1'} + k_1$ direction due to the time order of the excitation light. The diffracted signal intensity is proportional to $|P^{(3)}_{2k_2-k_{1'}} + P^{(3)}_{2k_2-k_1} + P^{(5)}_{2k_2-2k_1+k_{1'}}|^2$. The increase in the offset is due to the cross terms of the third- and fifth-order nonlinear polarizations, i.e., $P^{(3)}_{2k_2-k_{1'}} \times P^{(5)}_{2k_2-2k_1+k_{1'}}$ and

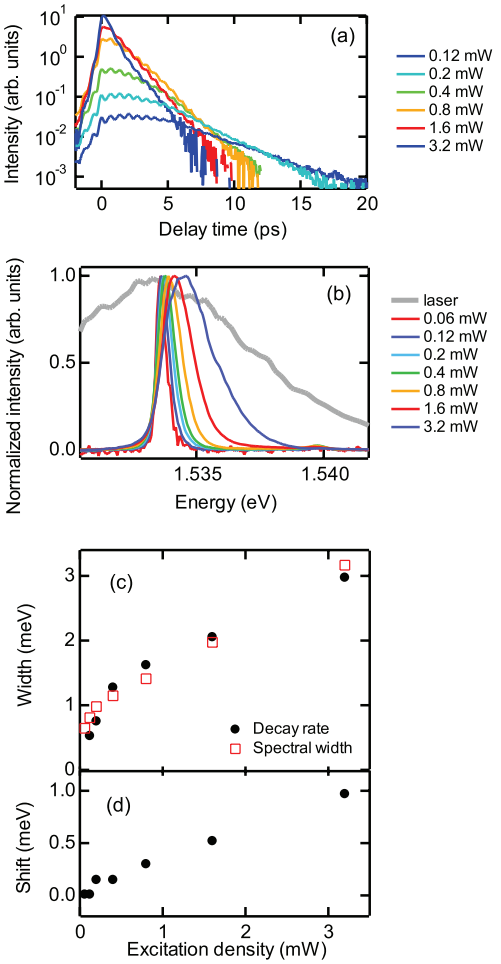

FIG. 2. (Color online) (a) Time-integrated and (b) spectrally resolved four-wave mixing intensity in co-circular configuration as a function of excitation density. The spectrum of excitation light is also presented. (c) Homogeneous width and (d) peak energy shift as a function of excitation density. Homogeneous width is estimated from decay rate [(a) solid circles] and spectral width [(b) open boxes].

$P^{(3)}_{2k_2-k_1} \times P^{(5)}_{2k_2-2k_1+k_{1'}}$, which are proportional to the fourth power of the excitation density.[23] Because the sign of the fifth-order nonlinear polarization is opposite to that of the third-order one, the oscillation of the offset is the reverse of the hh-lh quantum beat. On the other hand, there is no fifth-order signal in the RLV configuration because of the cross-circular polarization between the $k_{1'}$ and k_1 pulses. Therefore, the signal intensity is proportional to $|P^{(3)}_{2k_2-k_{1'}} + P^{(3)}_{2k_2-k_1}|^2$; the offset does not oscillate for the RLV configuration.

Although a change in decay rate is difficult to identify in Figs. 3(a) and 3(e), the decay rate changes depend on $t_{1'1}$ in the co-circular configuration. We estimated the homogeneous widths at various $t_{1'1}$ values from the exponential fittings of the decay curves; the homogeneous widths as a function of $t_{1'1}$ are shown in Fig. 4(a). As $t_{1'1}$ increases, the homogeneous width decays with the oscillation and has minima at $t_{1'1} = 0.33, 0.99$, 1.66, and 2.33 ps. It is expected that the homogeneous width decreases when the population of the hh (lh) exciton reduces and this population reduction leads to a suppression of the hh-hh (hh-lh) exciton scattering. We note that the homogeneous

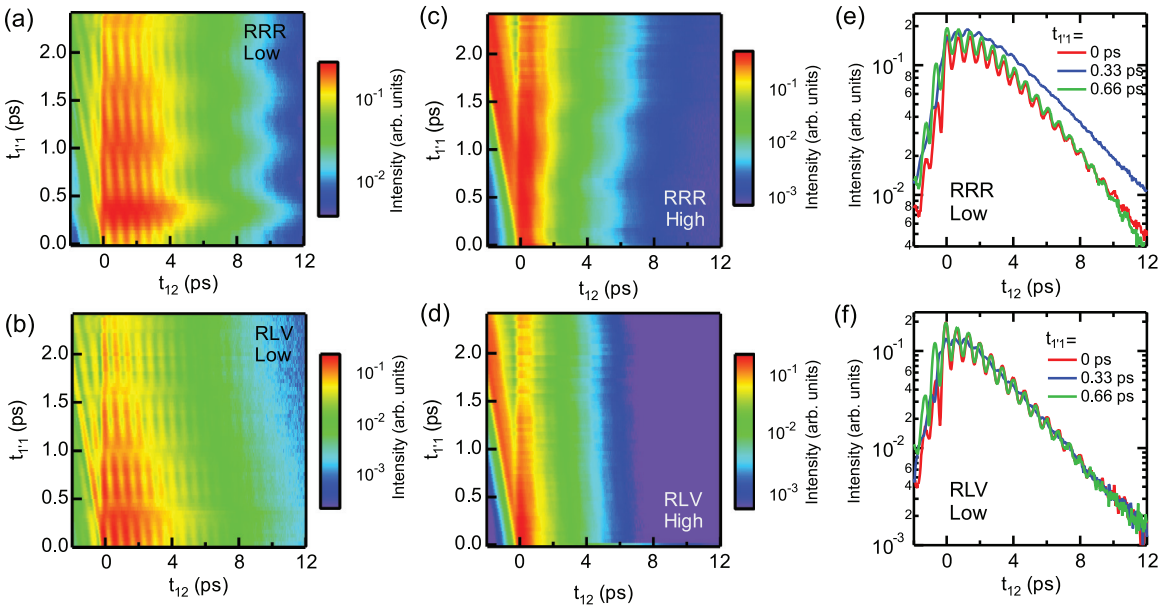

FIG. 3. (Color online) (a)–(d) Four-wave mixing intensity as a function of t_{12} and $t_{1'1}$ for co-circular (RRR) and cross-circular (RLV) configurations at low (0.12 mW) and high (1.2 mW) excitation densities. (e) and (f) Time-integrated FWM intensity at $t_{1'1} = 0$, 0.33, and 0.66 ps as a function of t_{12}.

width decreases around $t_{1'1} = 0$ ps, which is the result of the non-Markovian effect, as described below.

For simplicity we assume that the exciton polarization is driven in a homogeneous system by phase-locked pulses and that the k_2 pulse probes the created polarization. The scattering rates due to hh-hh and hh-lh exciton scatterings are calculated by using a weakly interacting boson model including the non-Markovian effect. Hereafter, the hh and lh excitons are abbreviated to X_h and X_l, respectively.

The origin of the scattering between excitons is Coulomb interaction that works instantaneously. The exciton-exciton interaction provides the energy shift of the exciton. The scattering occurs one after another and the exciton energy changes for each scattering. When the time scale of measurement is long enough, the power broadening is terminated at the moment when the excitation pulse disappears.

When the time scale of measurement is short enough, the energy shift is not random but depends on the history of the scattering. There is a correlation between energy shifts of exciton at different times due to the non-Markovian nature. The Hamiltonian of the X_h-X_h and X_h-X_l scatterings is written as

$$\hat{H}^{\mathrm{h,j}}_{\mathrm{scat}} = \frac{1}{2}\sum_{q\neq 0,k',k''}\int_0^\infty d\tau C_q^{\mathrm{h,j}}(\tau)\hat{b}^\dagger_{k''+q,\mathrm{h}}(t) \times \hat{b}^\dagger_{k'-q,\mathrm{j}}(t)\hat{b}_{k'',\mathrm{h}}(t-\tau)\hat{b}_{k',\mathrm{j}}(t-\tau) \quad (1)$$

by extending the Hamiltonian of the Markovian process.[19,24] Where $\hat{b}_{k,\mathrm{j}}$ is the annihilation operator for X_h (j = h) and X_l (j = l) with the wave vector k. The commutation relations for the exciton operators have the form $[\hat{b}_{k',\mathrm{j}'}(t-\tau),\hat{b}^\dagger_{k,\mathrm{j}}(t)] = \delta_{k'k}\delta_{\mathrm{j'j}}\exp[\mathrm{i}\omega_{\mathrm{j}}\tau]$, where $\hbar\omega_{\mathrm{j}}$ is the energy of X_h (j = h) and X_l (j = l). $C_q^{\mathrm{h,j}}(\tau)$ is the correlation function of the X_h-X_h (j = h) and X_h-X_l (j = l) scatterings. The correlation function of the non-Markovian scattering is phenomenologically represented by an exponential function similar to a linear Brownian motion, which is the result of the assumption that the fluctuation of exciton energy is linearly driven by the stochastic random force due to the exciton-exciton scattering.[25] On the other hand, the correlation function can be represented by a δ function in Markovian dynamics.

The scattering term due to the X_h-X_h scattering is expressed as

$$\frac{\partial}{\partial t}\langle\hat{b}_{k,\mathrm{h}}(t)\rangle\Big|^{\mathrm{h,h}}_{\mathrm{scat}} = \frac{\mathrm{i}}{\hbar}\langle[\hat{H}^{\mathrm{h,h}}_{\mathrm{scat}},\hat{b}_{k,\mathrm{h}}(t)]\rangle. \quad (2)$$

From Eqs. (1) and (2) we obtained

$$\frac{\partial}{\partial t}\langle\hat{b}_{k,\mathrm{h}}(t)\rangle\Big|^{\mathrm{h,h}}_{\mathrm{scat}} = -\frac{\mathrm{i}}{\hbar}\sum_{q\neq 0}\int_0^\infty d\tau C_q^{\mathrm{h,h}}(\tau) \times\langle\hat{b}^\dagger_{k+q,\mathrm{h}}(t)\hat{b}_{k+q,\mathrm{h}}(t-\tau)\hat{b}_{k,\mathrm{h}}(t-\tau)\rangle. \quad (3)$$

We decoupled the three-operator expectation value $\langle\hat{b}^\dagger_{k+q,\mathrm{h}}(t)\hat{b}_{k+q,\mathrm{h}}(t-\tau)\hat{b}_{k,\mathrm{h}}(t-\tau)\rangle$ by splitting it into a production of two-operator $\langle\hat{b}^\dagger_{k+q,\mathrm{h}}(t)\hat{b}_{k+q,\mathrm{h}}(t-\tau)\rangle$ and one-operator $\langle\hat{b}_{k,\mathrm{h}}(t-\tau)\rangle$ terms. The two-operator term is approximated as $\langle\hat{b}^\dagger_{k,\mathrm{h}}(t)\hat{b}_{k,\mathrm{h}}(t-\tau)\rangle$. The Heisenberg equations are written as

$$\frac{\partial}{\partial t}\langle\hat{b}_{k,\mathrm{h}}(t)\rangle = \frac{\mathrm{i}}{\hbar}\langle[\hat{H},\hat{b}_{k,\mathrm{h}}(t)]\rangle - \Gamma_2\langle\hat{b}_{k,\mathrm{h}}(t)\rangle, \quad (4)$$

$$\frac{\partial}{\partial t}\langle\hat{b}^\dagger_{k,\mathrm{h}}(t)\hat{b}_{k,\mathrm{h}}(t-\tau)\rangle = \frac{\mathrm{i}}{\hbar}\langle[\hat{H},\hat{b}^\dagger_{k,\mathrm{h}}(t)\hat{b}_{k,\mathrm{h}}(t-\tau)]\rangle, \quad (5)$$

$$\hat{H} = \hat{H}_0 + \hat{H}_{\mathrm{I}} + \hat{H}_{\mathrm{scat}}, \quad (6)$$

where $\hat{H}_0 = \sum_{k,\mathrm{j}}\hbar\omega_{\mathrm{j}}\hat{b}^\dagger_{k,\mathrm{j}}(t)\hat{b}_{k,\mathrm{j}}(t)$ is the nonperturbed Hamiltonian, $\hat{H}_{\mathrm{I}} = -\sum_{k,\mathrm{j}}\mu_{\mathrm{j}}\{E(t)\hat{b}^\dagger_{k,\mathrm{j}}(t) + E^*(t)\hat{b}_{k,\mathrm{j}}(t)\}$ is the interaction Hamiltonian between light and matter, and μ_{j} is the dipole moment of X_h (j = h) and X_l

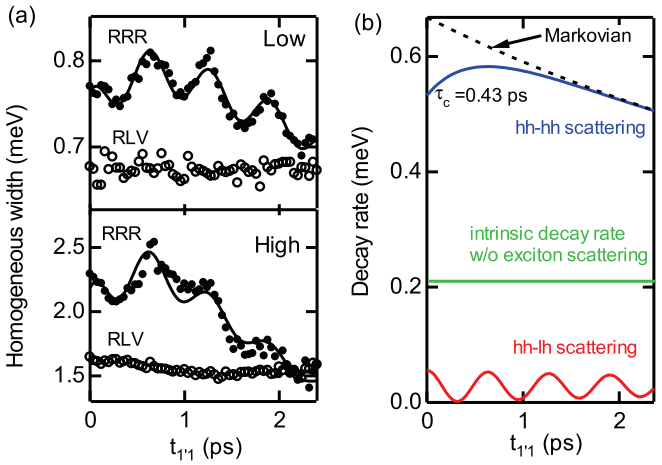

FIG. 4. (Color online) (a) Homogeneous widths as a function of $t_{1'1}$ obtained from the exponential fitting of the decay curves of the FWM signals for co-circular (RRR: solid circles) and cross-circular (RLV: open circles) configurations at low and high excitation densities. The solid line represents the calculated homogeneous width based on a weakly interacting boson model. (b) Calculated scattering rates as a function of $t_{1'1}$ for a co-circular configuration at low excitation density. The dashed line is the hh-hh exciton scattering term in the Markovian approximation. Details of the calculation are described in text. Correlation time of the hh-hh exciton scattering τ_c is 0.43 and 0.41 ps at low and high excitation densities, respectively.

(j = l). We added the intrinsic decay term Γ_2 at the zero-excitation density in Eq. (4). The driving electric field is expressed as $E(t) = \hbar\theta_{1'} \exp[-i\omega(t - t_{1'}) + ik_{1'}r]\delta_{k,k_{1'}}\delta(t - t_{1'}) + \hbar\theta_1 \exp[-i\omega(t - t_1) + ik_1 r]\delta_{k,k_1}\delta(t - t_1)$, where $\exp[-i\omega_h t_{1'1}] = 1$ because of the phase locking at the energy of X_h. Note that the excitation pulse is approximated by a δ function because the spectrum of the excitation pulse is much broader than the linewidth of excitons as shown in Fig. 2(b). To calculate Eqs. (4) and (5), we neglected the higher-order terms, i.e., the phase space filling term which leads to nonlinearity[24] and the scattering term $\hat{H}_{\rm scat}$. That is, the calculation is restricted to first order.

The scattering term is finally obtained as

$$\frac{\partial}{\partial t}\langle \hat{b}_{k,\rm h}(t)\rangle\Big|^{\rm h,h}_{\rm scat} = -\mu_{\rm h}^2 \frac{\rm i}{\hbar}\sum_{q\neq 0}\Bigg[\int_0^\infty d\tau C_q^{\rm h,h}(\tau) \times \left(\theta_{1'}^2 + \theta_1^2 + \theta_{1'}\theta_1 e^{-\Gamma_2 t_{1'1}}\right)e^{2i\omega_h\tau + 2\Gamma_2\tau} + \int_0^{t_{1'1}} d\tau C_q^{\rm h,h}(\tau)\theta_{1'}\theta_1 e^{-\Gamma_2 t_{1'1}} \times e^{2i\omega_h\tau + 2\Gamma_2\tau}\Bigg]\langle \hat{b}_{k,\rm h}(t)\rangle, \quad (7)$$

for a sufficiently large t. The real part of the coefficient of $\langle \hat{b}_{k,\rm h}(t)\rangle$ in the RHS is the decay rate due to the X_h-X_h scattering. The $\theta_{1'}^2$ and θ_1^2 terms indicate the power broadening by the $k_{1'}$ and k_1 pulses, respectively, and are proportional to the excitation density. The two $\theta_{1'}\theta_1$ terms in the second and third lines represent the cross correlation after and before the arrival of the second pulse, respectively. The cross-correlation terms disappear in the cross-circular configuration. Therefore, the homogeneous width does not depend on $t_{1'1}$ in the RLV configuration, as shown in Fig. 4(a). Although exciton-free carrier scattering is one of the main decoherence channels,[26] we omit the contribution of the exciton-free carrier scattering because the free carrier is not controlled by the irradiation of the phase-locked pulses. If the relative phase of the phase-locked pulses is δ, then $-\Gamma_2 t_{1'1}$ is replaced by $-\Gamma_2 t_{1'1} + i\delta$. The relative phase dependence of the decay rate has been reported for a ZnSe SQW.[27]

The scattering term due to the X_h-X_l scattering is calculated by the same procedure:

$$\frac{\partial}{\partial t}\langle \hat{b}_{k,\rm h}(t)\rangle\Big|^{\rm h,l}_{\rm scat} = -\mu_{\rm l}^2 \frac{\rm i}{2\hbar}\sum_{q\neq 0}\Bigg[\int_0^\infty d\tau C_q^{\rm h,l}(\tau)\left(\theta_{1'}^2 + \theta_1^2 + \theta_{1'}\theta_1 e^{i\Delta\omega t_{1'1} - \Gamma_2 t_{1'1}}\right)e^{i(2\omega_h + \Delta\omega)\tau + 2\Gamma_2\tau} + \int_0^{t_{1'1}} d\tau C_q^{\rm h,l}(\tau)\theta_{1'}\theta_1 e^{-i\Delta\omega t_{1'1} - \Gamma_2 t_{1'1}} \times e^{i(2\omega_h + \Delta\omega)\tau + 2\Gamma_2\tau}\Bigg]\langle \hat{b}_{k,\rm h}(t)\rangle, \quad (8)$$

where $\hbar\Delta\omega$ is the energy difference between X_h and X_l. The total decay rate is determined by the X_h-X_h and X_h-X_l scattering, and the intrinsic decay rate Γ_2.

In the Markovian approximation, the correlation function is given by the δ function as described above, for example, $\sum_{q\neq 0} C_q^{\rm h,h}(\tau) = C^{\rm h,h}(0)\delta(\tau)$. Therefore, the decay rates due to the X_h-X_h and X_h-X_l scatterings are proportional, respectively, to the population of X_h and X_l, i.e., $\mu_h^2(\theta_{1'}^2 + \theta_1^2 + 2\theta_{1'}\theta_1 \exp[-\Gamma_2 t_{1'1}])$ and $\mu_l^2(\theta_{1'}^2 + \theta_1^2 + 2\theta_{1'}\theta_1 \cos[\Delta\omega t_{1'1}]\exp[-\Gamma_2 t_{1'1}])$. The population of X_h is constructively generated by the phase-locked pulses when the delay time is smaller than the dephasing time. The population of X_l oscillates with the period of $2\pi/\Delta\omega$, due to the phase locking at the energy of X_h.[28]

In the non-Markovian dynamics, the correlation function is written as $\sum_{q\neq 0} C_q^{\rm h,j}(\tau) = C^{\rm h,j}(0)\exp[-\Gamma_c\tau]$, where j = h, l, and Γ_c is the inverse of the correlation time τ_c. The $t_{1'1}$ dependence of the homogeneous width is well reproduced by the above model, as denoted by the solid line in Fig. 4(a). We neglected the non-Markovian effect of the X_h-X_l scattering because its contribution to the decay rate is small. The excitation density $\theta_{1'}$ is equal to θ_1, from the experimental condition. The calculated scattering terms due to the X_h-X_h and X_h-X_l scatterings, and the intrinsic decay rate are described in Fig. 4(b). The X_h-X_l scattering term oscillates with $t_{1'1}$ depending on the population of X_l. The dashed line in Fig. 4(b) is the X_h-X_h scattering term in the Markovian approximation, which is proportional to the population of X_h.

The decrease in the X_h-X_h scattering around $t_{1'1} = 0$ ps is caused by the non-Markovian effect. As mentioned above, there is a correlation between energy shifts of exciton at different times during the correlation time. That is, the past energy shifts influence the present dynamics. When a pulse pair is incident, there is no distinction between excitons generated by first and second pulses. Thus, the power broadening due to the cross correlation exists within the correlation time before and after the arrival of the second pulse. If the temporal separation of the pulse pair is shorter than the correlation time, the power broadening decreases because the

cross-correlated scattering does not occur before the arrival of the first pulse because of the *causality*. This effect is represented by the upper limit of the integral of the third line of Eq. (7). Therefore, the X_h-X_h scattering decreases around $t_{1'1} = 0$ ps; the correlation time τ_c is estimated as 0.43 ps. We note that the cross-correlated power broadening also exits after the arrival of the second pulse; it shows the exponential decay with decay rate Γ_2 as described in the $\theta_{1'}\theta_1$ term of the second line of Eq. (7).

Even with a tenfold increase in the excitation density, the correlation time varies only within the margin of error [see Fig. 4(a)], despite the decrease in dephasing time. In a dense potassium vapor, the correlation time due to dipole-dipole interaction between excited and unexcited atoms decreases with increasing the density.[29] The weak excitation density dependence in the GaAs SQW is expected to be because of the screening of the Coulomb interaction due to the large dielectric constant in condensed matter.

The correlation time of the exciton-exciton scattering has been reported for a ZnSe SQW.[19] The correlation time has been experimentally obtained as 0.54 ps by monitoring the shape change of the FWM spectra; this estimated value is close to our results. In addition, the presence of a long time tail in the correlation function has been demonstrated by microscopic calculations. However, we cannot discuss the presence of the long time tail in the GaAs SQW, because the change of the FWM spectra shape had not been observed in our experiment.

From the amplitude of the hh-lh quantum beat at a low excitation density [Fig. 3(a)], the ratio of the population of X_l and X_h, $\mu_l^2\theta_l^2/\mu_h^2\theta_h^2$, is estimated as 0.12, where θ_l^2 and θ_h^2 are the excitation densities at the resonance of X_l and X_h. In addition, from the fitting results in Fig. 4(b), the ratio of the decay rate due to the X_h-X_l and X_h-X_h scatterings, $\mu_l^2\theta_l^2\mathrm{Re}[C^{h,l}(0)]/2\mu_h^2\theta_h^2\mathrm{Re}[C^{h,h}(0)]$, is 0.062. Consequently, we can find that $\mathrm{Re}[C^{h,l}(0)] \sim \mathrm{Re}[C^{h,h}(0)]$. Due to the same charge structure of X_h and X_l, the dipole-dipole interaction between X_h and X_h is corresponding to that between X_h and X_l.

In conclusion, we have shown that the exciton-exciton scattering can be controlled by the irradiation of phase-locked pulses. The non-Markovian effect of the scattering is well reproduced by the theoretical model calculation. In this work we have discussed the two-particle correlation and the correlation time. By applying the coherent control technique to higher-order nonlinear optical spectroscopy, such as six-wave mixing,[30] and by using two-dimensional Fourier transform spectroscopy,[31] the non-Markovian effect of higher-order correlation among excitons can be investigated.

The authors acknowledge financial support from a Grant-in-Aid for Scientific Research on Innovative Areas (KAKENHI 23104711) and the Global Center of Excellence Program by MEXT, Japan, through the Nanoscience and Quantum Physics Project of the Tokyo Institute of Technology.

[1] D. S. Chemla and J. Shah, Nature (London) **411**, 549 (2001).
[2] D. J. Lovering, R. T. Phillips, G. J. Denton, and G. W. Smith, Phys. Rev. Lett. **68**, 1880 (1992).
[3] J. Shah, M. Combescot, and A. H. Dayem, Phys. Rev. Lett. **38**, 1497 (1977).
[4] For a review, A. Griffin, D. W. Snoke, and S. Stringari, *Bose-Einstein Condensation* (Cambridge University Press, Cambridge, 1995).
[5] H. Haug and S. W. Koch, *Quantum Theory of the Optical and Electronic Properties of Semiconductors* (World Scientific, Singapore, 2009).
[6] V. M. Axt and S. Mukamel, Rev. Mod. Phys. **70**, 145 (1998).
[7] L. Banyai, D. B. Tran Thoai, E. Reitsamer, H. Haug, D. Steinbach, M. U. Wehner, M. Wegener, T. Marschner, W. Stolz, Phys. Rev. Lett. **75**, 2188 (1995).
[8] M. U. Wehner, D. S. Chemla, and M. Wegener, Phys. Rev. B **58**, 3590 (1998).
[9] M. U. Wehner, M. H. Ulm, D. S. Chemla, and M. Wegener, Phys. Rev. Lett. **80**, 1992 (1998).
[10] D. Steinbach, G. Kocherscheidt, M. U. Wehner, H. Kalt, M. Wegener, K. Ohkawa, D. Hommel, and V. M. Axt, Phys. Rev. B **60**, 12079 (1999).
[11] U. Woggon, F. Gindele, W. Langbein, and J. M. Hvam, Phys. Rev. B **61**, 1935 (2000).
[12] H. J. Bakker, K. Leo, J. Shah, and K. Köhler, Phys. Rev. B **49**, 8249 (1994).
[13] Y. Ogawa, A. Iwamatsu, and F. Minami, Phys. Rev. B **73**, 153203 (2006).
[14] T. Kishimoto, A. Hasegawa, Y. Mitsumori, J. Ishi-Hayase, M. Sasaki, and F. Minami, Phys. Rev. B **74**, 073202 (2006).
[15] S. G. Carter, Z. Chen, and S. T. Cundiff, Phys. Rev. B **76**, 121303(R) (2007).
[16] H. Tahara, Y. Ogawa, and F. Minami, Phys. Rev. B **82**, 113201 (2010).
[17] H. Tahara, Y. Ogawa, and F. Minami, Phys. Rev. Lett. **107**, 037402 (2011).
[18] P. Borri, W. Langbein, S. Schneider, U. Woggon, R. L. Sellin, D. Ouyang, and D. Bimberg, Phys. Rev. Lett. **87**, 157401 (2001).
[19] V. M. Axt, T. Kuhn, B. Haase, U. Neukirch, and J. Gutowski, Phys. Rev. Lett. **93**, 127402 (2004).
[20] J. Shah, *Ultrafast Spectroscopy of Semiconductors and Semiconductor Nanostructures*, 2nd ed. (Springer, Berlin, 1999).
[21] G. Manzke, Q. Y. Peng, K. Henneberger, U. Neukirch, K. Hauke, K. Wundke, J. Gutowski, and D. Hommel, Phys. Rev. Lett. **80**, 4943 (1998).
[22] D. R. Wake, H. W. Yoon, J. P. Wolfe, and H. Morkoç, Phys. Rev. B **46**, 13452 (1992).
[23] Y. Ogawa, F. Minami, and N. Yamamoto, J. Lumin. **129**, 1817 (2009).
[24] M. Kuwata-Gonokami, S. Inouye, H. Suzuura, M. Shirane, R. Shimano, T. Someya, and H. Sakaki, Phys. Rev. Lett. **79**, 1341 (1997).
[25] S. Mukamel, *Principles of Nonlinear Optical Spectroscopy* (Oxford University Press, Oxford, 1995).

[26] A. Honold, L. Schultheis, J. Kuhl, and C. W. Tu, Phys. Rev. B **40**, 6442 (1989).
[27] T. Voss, H. G. Breunig, I. Rückmann, and J. Gutowski, Phys. Rev. B **69**, 205318 (2004).
[28] A. P. Heberle, J. J. Baumberg, and K. Köhler, Phys. Rev. Lett. **75**, 2598 (1995).
[29] V. O. Lorenz and S. T. Cundiff, Phys. Rev. Lett. **95**, 163601 (2005).
[30] S. R. Bolton, U. Neukirch, L. J. Sham, D. S. Chemla, and V. M. Axt, Phys. Rev. Lett. **85**, 2002 (2000).
[31] X. Li, T. Zhang, C. N. Borca, and S. T. Cundiff, Phys. Rev. Lett. **96**, 057406 (2006).